Desalination and Water Treatment
www.deswater.com

doi:10.5004/dwt.2018.22352

125 (2018) 227–234
September

Variation of total dissolved iron and its impacts during an extreme flooding event in a boreal forest catchment

Jia Wang[†], Jiunian Guan[†], Liu Yang, Zirui Wang, Nan Lu*, Ying Lu*

School of Environment, Northeast Normal University, No. 2555, Jingyue Street, 130117 Changchun, China, email: 1097061048@qq.com (J. Wang), guanjn461@nenu.edu.cn (J. Guan), lun100@nenu.edu.cn (N. Lu), luy332@nenu.edu.cn (Y. Lu)

Received 24 February 2018; Accepted 6 April 2018

ABSTRACT

The extreme flooding event (EFE) acts as the essential role in the export of riverine total dissolved iron (TDFe) which limits primary productivity in marine ecosystems. In order to reveal the influence of EFE on the variation of TDFe, water samples were collected in the Yalu River, as a typical boreal forest catchment in China, to analyze TDFe concentration and speciation as well as relevant water quality parameters during EFE together with regular flood season (RFS) and base flow period (BFP). The results indicated TDFe concentration represented a significant increase trend during EFE, with an average concentration of 0.24 mg/L. The TDFe species was dominated by Fe(III) in low-molecular-weight by filtration and ultra filtration methods. The impulse of TDFe concentration during EFE can be attributed to the hydrological connection to the riparian wetlands and intensive territorial runoff. The correlation analysis indicated that dissolved organic matter (DOM) with high values of high humification degree (HIX) served as the crucial chelation of Fe(III). Furthermore, the dynamics and migration of TDFe and DOM may potentially influence the water quality in the catchment via altering the transport of nutrients and trace metals, which merits closer attention at the background of global climate changes.

Keywords: Dissolved organic matter; Fe-DOM complexes; Forest; Humification index; Hydrological connection; Wetland

1. Introduction

As one of the most abundant element in the Earth's crust, iron (Fe) widely exists in different aquatic ecosystems, participating in various ecological and physiological processes, such as photosynthesis, biological nitrogen fixation, and biomass production [1]. Recently, there has been an increasing concern on the variation of riverine total dissolved iron (TDFe) output to the ocean due to its function in controlling the primary production in the marine ecosystems known as high-nitrate and low-chlorophyll (HNLC) regions [2–4]. The Okhotsk Sea, unlike other HNLC region of Northern Pacific, is characterized by high phytoplankton productivity owing to the sufficient inputs of TDFe from the Amur River [5]. As a consequence, researches on the biogeochemical cycling of Fe has been a hot spot in this boreal river basin [6,7]. Our previous researches have revealed that the Songhua River, as the largest tributary of Amur River, played a critical role in export of TDFe [8,9]. However, as an important landscape in the Songhua River basin, it is still rarely reported regarding to the concentration and speciation of TDFe in the boreal forest catchments in the basin.

As a link between territorial and aquatic ecosystems, dissolved organic matter (DOM) is a fundamental constituent that influences biogeochemical cycling of Fe serving as the most principal ligand and transport vector in boreal rivers [10,11]. In freshwater, Fe(II) can be rapidly oxidized to Fe(III) and precipitate as Fe oxyhydroxides; whereas due to the affinity of DOM for Fe, a large quantity of Fe is complexed with DOM in equilibrium with Fe (oxy) hydrox-

---

*Corresponding author.

[†]These authors contributed equally to this work

Presented at the 4th Annual Science and Technology Conference (Tesseract'17) at the School of Petroleum Technology, Pandit Deen Dayal Petroleum University, 10-12 November 2017, Gandhinagar, India

1944-3994 / 1944-3986 © 2018 Desalination Publications. All rights reserved.

ides in boreal rivers [12]. DOM is a heterogeneous complex of organic compounds, different quality (e.g. molecular weight, humification degree, aromaticity etc.) exhibits different properties in binding Fe, which further influences its solubility, stability and bioavailability. However, it remains virtually unknown that the chemical structure of Fe-DOM complexes represented by soil fulvic DOM or autochthonous microbial exometabolites and its transformation products [13]. Therefore, to further reveal the biogeochemical properties of Fe-DOM complexes, it causes pressure to reveal the links between TDFe and DOM quality in boreal aquatic environments.

Owing to global climate change, the recession rate of flooding event has been enhanced coupled with frequently occurred rainstorm in boreal region, becoming an important explanation of increasing TDFe output in the boreal rivers and streams over recent decades, which is also the case for the Songhua River [14–17]. It is well-established that the flooding event exerted a dominant influence on the export of riverine TDFe, while the hydrological connectivity between Fe sources and the surface water draining the catchment controls TDFe flux, likewise DOM [8,18,19]. Therefore, it is crucial to determine variations in the concentration and speciation of TDFe and the significance of its environmental impact on the boreal catchments during the flooding event.

In 2013, an extreme flooding event (EFE) induced by intensive and prolonged rainfall occurred in the Yalu River, a typical boreal forest catchment in the Songhua River Basin. Thus, this study presents the relevant data monitored during this event, together with regular flood season (RFS) and base flow period (BFP) in 2014 and 2015, with the following aims: (i) to reveal the variation of TDFe concentration and speciation during EFE; (ii) to investigate the origin of TDFe; and (iii) to discuss its potential environmental impact on the water quality.

2. Methodology

2.1. Study area

The Yalu River is one of the main tributaries of the upper Songhua River (Nenjiang River), with a length of 398 km. The river basin (47°53′–48°52′N, 121°25′–122°52′E), covering 20,600 km^2 (Fig. 1). The basin at the upstream areas of Zhalantun is mainly composed of forests and wetlands, accounting for over 75% and 12% of the basin area, respectively (Table 1), where the complex mosaic of forests and scattered wetlands is characterized by organically rich soils that are traversed by network of rivers and streams. Whereas the anthropogenic interference in the basin is relatively limited with no more than 10% of the basin area as farmland and residential area. The annual average temperature varied between –5°C and 4°C, with an average frozen period of 130 days from November to April in the next year. The annual precipitation fluctuates from 420 mm to 480 mm, 65–75% of which occurs from June to August and the rainstorm center usually located around Zhalantun City. According to the monthly runoff (Fig. 2), RFS consists of July and August, taking account

Table 1
The landscape elements of the Yalu River catchment

Landscape	Area (km^2)	Proportion (%)
Forests	5206	75.8
Wetlands	872	12.7
Farmland	519	7.6
Meadow	193	2.8
Residential area	80	1.2
Total	6870	100

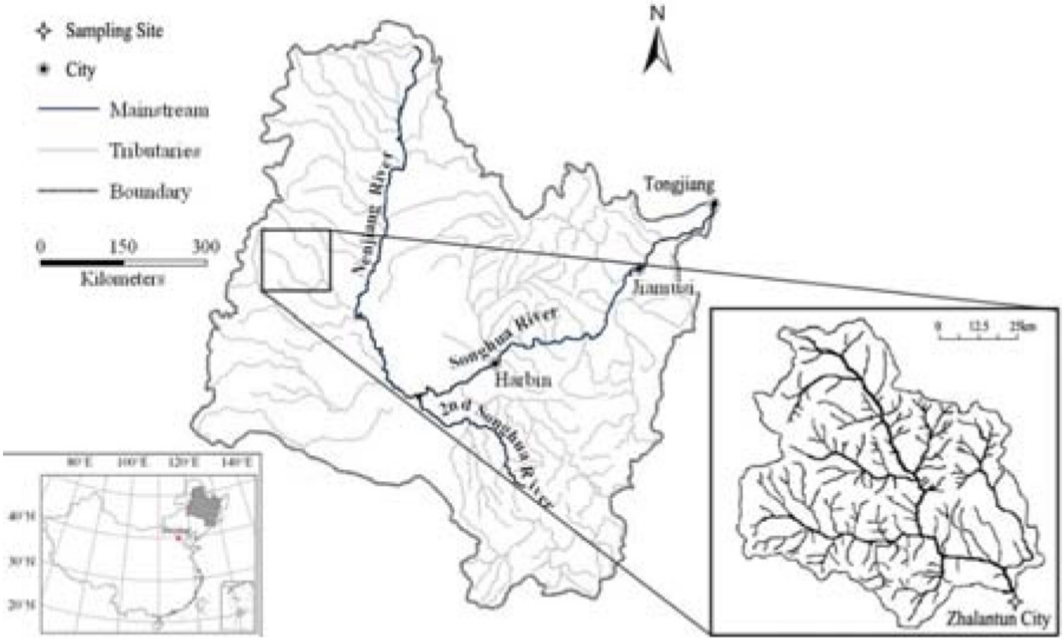

Fig. 1. The location of sampling sites.

for 56% of the annual runoff with an average of 2.32 billion m^3; whereas BFP comprises May, June, and October in the current study.

In 2013, an extreme flooding event occurred in the Songhua River Basin with an average precipitation of 459 mm, which was 30% more than the average value (352 mm). Meanwhile, the precipitation achieved 563.7 mm in the Nenjiang River Basin, which was approximately 40% more than the average value of 406.8 mm. The associated flooding resulted in an over 50-year return in the Nenjiang River and the second severed flooding event ever recorded in the Yalu River. While in both 2014 and 2015, the river was in a regular hydrological condition.

2.2. Sample collection

Water samples were collected according to standard methods from Water Quality-Technical Regulation on the Design of Sampling Programs (HJ 495-2009, China EPA) at the Yaluhe Bridge (48°00′30″N, 122°42′56″ E) in Zhalantun City, during EFE from July to September in 2013, RFS in 2014 and 2015, as well as BFP from 2013 to 2015. The collected water sample of 2.0 L were immediately stored in a portable refrigerator (4°C) and transported to the laboratory for further treatment and analysis.

2.3. Sample analysis

In the current study, fractions of TDFe were determined by the ultra filtration method (i.e. cross-flow filtration, CFF) established in our previous researches [8,20]. The recovery rate was 94.7–104.2% with a detection limit of 0.002 mg/L. Fe(II) concentration were measured using an ET7406 Fe Tester (Lovibond, Dortmund, Germany) with o-Phenanthroline spectrophotometric method *in situ* and Fe(III) concentration were calculated as the difference between LMWFe and Fe(II) [21]. The concentrations of other Fe speciation as well as Mn were determined by a flame atomic absorption spectrophotometer (GBC 932, GBC Scientific Equipment Pty, Ltd, Braeside, Australia). Dissolved organic carbon (DOC) was analyzed using a TOC-V$_{CPH}$ (SHIMADZU, Kyoto, Japan). The concentrations of ammonium (NH_4^+-N), nitrate (NO_3^--N), phosphate phosphorus (PO_4^{3-}-P) in each sample were measured using a discrete auto analyser (Mode Smartchem 200, AMS, Rome, Italy).

The indices of humification index (HIX) and biological index (BIX) were obtained by a fluorescence spectrophotometer (Cary Eclipse, Varian, Palo Alto, USA) with a scan speed of 600 nm/min and a slit of 5 nm. HIX was defined as the ratio of the area under the emission spectra between the quarter (Σ435–480 nm) and (Σ300–345 nm) at λ_{ex} = 254 nm [22,23]; BIX was defined as the ratio of two fluorescence intensities (i.e. the intensity ratio of $I_{\lambda em=380}/I_{\lambda em=430}$) at λ_{ex} = 310 nm [24].

2.4. Data analysis

Statistical analysis and linear regression were conducted using SPSS 23.0 statistical software (SPSS Inc., Chicago, USA). Spearman correlation analysis was performed to analyze the correlation between different Fe speciation and other parameters since all the data did not show a normal distribution pattern by *Q-Q* probability plot analysis. One-way analysis of variance (ANOVA) was performed to compare the differences of data monitored during different periods. The difference was considered significant if $P < 0.05$.

3. Results and discussion

3.1. Parameter set of DOM and basic aquatic quality

During EFE, DOC values increased significantly ($P < 0.01$) compared with RFS (averaged at 4.21 mg/L) and BFP (averaged at 3.37 mg/L), fluctuating from 5.08 mg/L to 8.42 mg/L with an average of 7.17 mg/L (Table 2). On the basis of the increase in the C/H ratio, the maturation extent of DOM was determined by HIX which is also employed to investigate the humification degree, aromaticity, molecular weight as well as bioavailability of DOM within natural system. HIX values of the water samples in the current study mainly fluctuated in a range from 6 to 12, indicating DOM has an important terrestrial originated humic character while a weak recent autochthonous component [22,23]. Compared with BFP, HIX increased during EFE and RFS due to enhanced inputs of terrestrial DOM characterized by an increasing humification degree, molecular weight as well as aromaticity, which were consistent with the previous studies in other rivers [25–27]. BIX was recently proposed to assess the relative contribution of autochthonous DOM. In the current study, the values of BIX varied around 0.6 without seasonal variation, even during EFE, demonstrating the limited autochthonous component of DOM, which was agreed with other studies [28,29]. To sum up, the quality indices showed a predominance of terrestrial origins in DOM chemical composition, with significant fluctuations during EFE due to the alteration of DOM sources in the catchment.

The water quality was fit for the grade-III surface water criterion according to the Environmental Quality Standard for Surface Water (GB3838-2002, China EPA) during all the monitored periods. During EFE, the concentrations of nutrients including NH_4^+-N, NO_3^--N and PO_4^{3-}-P averaged 0.12, 0.98 and 0.08 mg/L, respectively, which also demonstrated a trend of significant increase ($P < 0.01$) compared with those during both RFS and BFP (Table 2), due to the integration of nutrients from different sources into the catchment via storm runoff [30]. However, the values of Mn concentrations maintained steadily among all these periods ($P > 0.05$).

3.2. The variations of TDFe concentrations during EFE

During EFE, the concentrations of TDFe fluctuated from 0.12 mg/L to 0.31 mg/L with a mean value of 0.24 mg/L, representing a significant increase ($P < 0.01$) compared with those (0.16 mg/L–0.28 mg/L, mean 0.20 mg/L) during NSP (Fig. 3). The minimum level of TDFe concentrations was observed during BFP, varying between 0.10 mg/L and 0.25 mg/L averaged at 0.15 mg/L.

It was documented that TDFe concentration was 0.14 ± 0.25 mg/L during flood season and 0.07 ± 0.09 mg/L during low water period in eastern China rivers [31]. By

Table 2
The aquatic quality parameters in the Yalu River

Period	Statistics	DOC	NH_4^+-N	NO_3^--N	PO_4^{3-}-P	Mn	BIX	HIX
		mg/L	mg/L	mg/L	mg/L	mg/L		
EFE (N=54)	Range	5.08–8.42	0.05–0.22	0.31–1.98	0.01–0.15	0.01–0.05	0.53–0.65	6.22–11.76
	Mean ± SD	7.17 ± 0.93	0.12 ± 0.05	0.91 ± 0.46	0.08 ± 0.05	0.03 ± 0.01	0.58 ± 0.05	9.69 ± 1.82
RFS (N=45)	Range	3.03–5.88	0.03–0.13	0.40–1.08	0.01–0.08	0.02–0.06	0.55–0.64	5.08–9.12
	Mean ± SD	4.21 ± 1.12	0.06 ± 0.03	0.64 ± 0.21	0.05 ± 0.03	0.04 ± 0.01	0.59 ± 0.03	7.11 ± 1.46
BFP (N=30)	Range	1.83–5.75	0.05–0.16	0.22–0.68	0.01–0.05	0.03–0.05	0.58–0.66	5.67–8.12
	Mean ± SD	3.37 ± 1.18	0.08 ± 0.05	0.44 ± 0.27	0.02 ± 0.02	0.04 ± 0.01	0.61 ± 0.04	6.76 ± 1.26

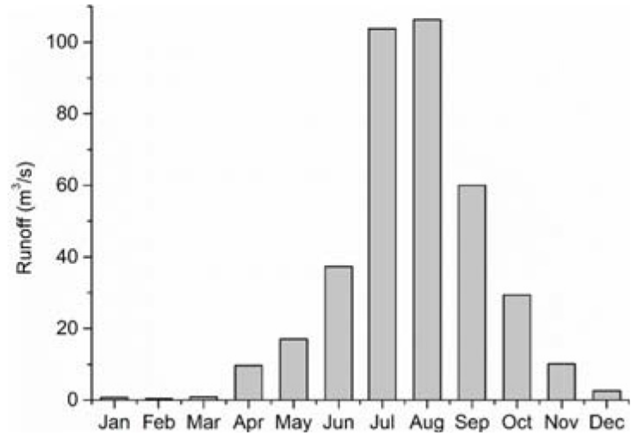

Fig. 2. Average monthly runoff of the Yalu River at Zhalantun City.

comparison, TDFe content in the Yalu River was at a relatively high level, which is in line with that the boreal rivers are commonly characterized by a high TDFe content [32]. This may be attributed to the geological conditions of the catchment filled with iron-rich terrigenous sedimentary, volcanogenic and intrusive rocks (Fe contents range from 3% to 6%) as well as soils (available Fe contents vary from 3% to 5%). Furthermore, it is a common feature that TDFe concentrations in rivers may remarkably correlate to the discharge in association with precipitation intensity and amount [33,34]. As a consequence, the territorial runoff during EFE can drive soil erosion and leaching, carrying a huge amount of iron-rich fine soil particles into the receiving river and enhancing the activation and release of TDFe [35,36]. Moreover, during the flooding event, it is the hydrological connectivity between the biogeochemical sources of Fe and surface water that is of fundamental importance for deciphering the pattern and dynamics of TDFe [37,38]. A high accumulation of TDFe has been documented in both wetland soils and surface water in boreal wetlands 20, which are intensively distributed in the riparian zones of the Yalu River. Hence, the riparian wetlands donated a significance of TDFe to the river via buffering the flood during EFE; whereas, it may be isolated to the river during BFP, limiting the export of TDFe [39].

Nevertheless, compared with TDFe concentrations averaged at 0.69 mg/L in the mainstream of the Songhua Rive during the current EFE in 2013 [16], the forest catchment did not contribute TDFe to a large extent, which may be attributed to the relatively low share of wetlands in the basin of Yalu River, together with restraining the intensity of territorial runoff by the vegetation in the forests.

3.3. The variations of TDFe species during EFE

Based on the molecular size, TDFe existed primarily in the species of LMW, the relative proportions of TDFe species varied according to the order LMWFe > HMWFe > MMWFe during each monitored period (Fig. 2). Fe(III) was the dominant speciation during all the monitored periods, whose proportion increased significantly during EFE (62.5%) and RFS (61.0%), compared with that during BFP (50.4%).

A remarkable correlation between DOC and TDFe ($P < 0.01$) was observed during both EFE and RFS (Fig. 4), whereas it was not the case during BFP ($P > 0.05$), intimating the important function of DOM on TDFe export and migration during the flooding season/event. Moreover, a significantly positive correlation between Fe(III) and HIX ($P < 0.01$) was obtained during both EFE and RFS (Fig. 5), indicating that fulvic DOM with high molecular weight, aromaticity and large size fractions may be the crucial chelation of Fe(III) and contribute largely in forming Fe(III)-DOM complexes, due to the high density of carboxylate functional groups which have high selectivity and affinity for Fe(III) [40]. Additionally, it was documented that the molecular size of TDFe in the wetland surface water was in the same pattern as that observed in the current study, whereas DOM from the territorial runoff under the forests may not be as enriched in aromatic, high molecular weight humic-like organic compounds as that in the wetland due to its relatively low values of HIX, confirming that the wetlands may be the crucial source of TDFe in the Yalu River [41–43]. Furthermore, the complexation of Fe(III) to fulvic DOM may reduce its bioavailability via inhibiting enzymatic processes and the generated Fe(III)-DOM complexes are generally considered to be transported over longer distance compared with Fe (oxy) hydroxides that are more likely to aggregate and settle [44]. It may further influence the downstream water quality via altering environmental processes and ecotoxicity of the pollutants that associated with Fe (oxy) hydroxides.

In the context of global climate change, the intensification of precipitation and flooding event would result in

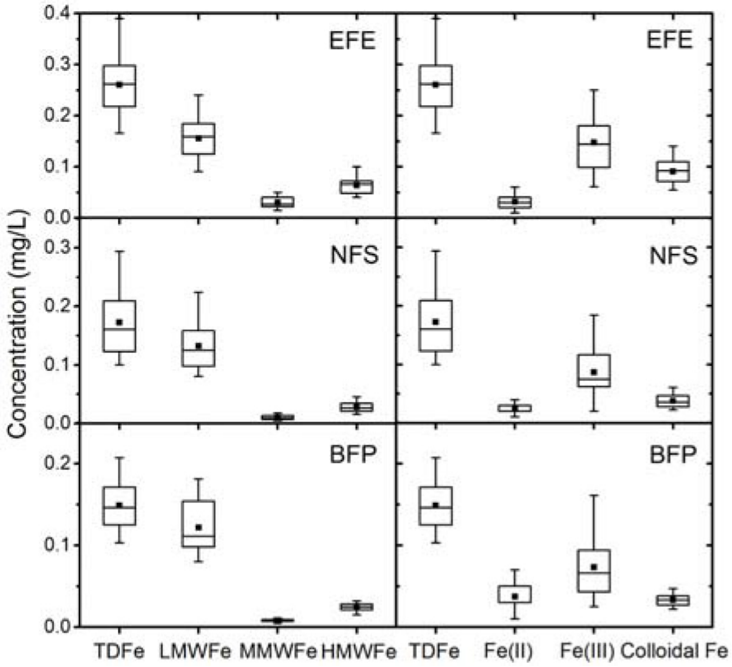

Fig. 3. Variation of TDFe concentration and speciation during different periods.

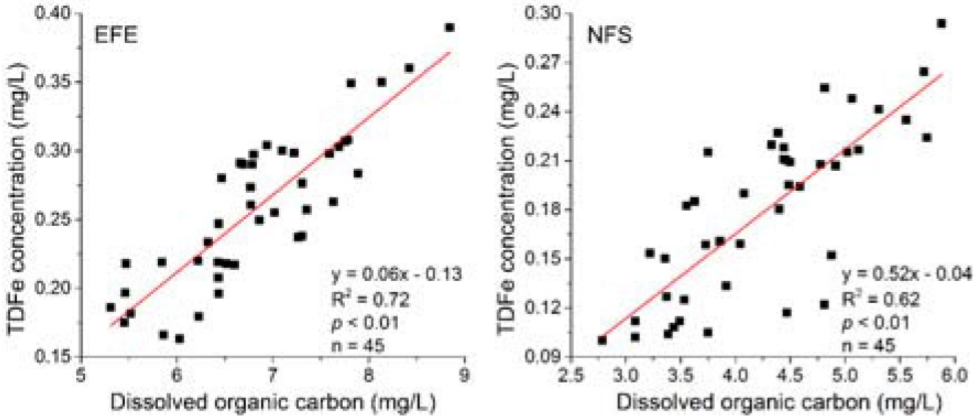

Fig. 4. Linear regression of total dissolved iron and dissolved organic carbon.

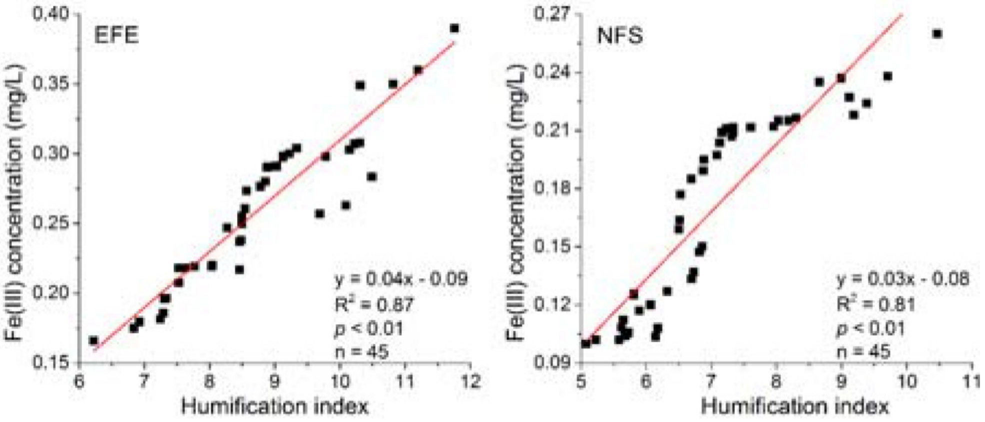

Fig. 5. Linear regression of Fe(III) and humification index.

Table 3
Spearman correlation of aquatic parameters

	Period	DOC	NH_4^+-N	NO_3^--N	PO_4^{3-}-P	Mn
Fe(II)	EFE (n=54)	-0.40^b		-0.47^b		
Fe(III)		0.87^a		0.69^a	0.77^a	
Colloidal Fe					0.46^b	0.64^a
TDFe		0.72^a			0.69^a	0.49^b
Fe(II)	RFS (n=45)		0.56^a			
Fe(III)		0.81^a		0.55^a	0.67^a	0.67^a
Colloidal Fe		0.42^b				
TDFe		0.62^a			0.54^a	0.56^a
Fe(II)	BFP (n=30)					
Fe(III)		0.57^a		0.46^b	0.47^b	
Colloidal Fe						0.52^b
TDFe					0.57^a	

a. Correlation is significant at the 0.01 level (2-tailed).
b. Correlation is significant at the 0.05 level (2-tailed).

the reinforcement of TDFe migration and dynamics in the boreal catchments, providing a crucial sequence of nutrient cycling in the catchments [45,46]. In the current study, a significant positive correlation was observed between Fe(III) and PO_4^{3-}-P (Table 3), suggesting the formation of coordination complexes of Fe-DOM can also absorb phosphate in water column [47,48]. Moreover, Fe(III) also positively correlated with NO_3^--N, since bacteria can take Fe(III) as electron acceptor to produce energy by oxidizing NH_4^+-N into NO_3^--N [49]. Thus, the variations of TDFe concentration and speciation during EFE may promote the release of nutrient elements from the sediment-water interface and riparian zones, which would consequently have potential impacts on the water quality and aquatic ecosystem such as eutrophication.

The synchronous impulse of TDFe and DOM during EFE resulted in the generation of stabilized Fe(III)-DOM complexes, which suppressed Fe (oxy)hydroxides precipitation, even at neutral pH values, which may enhance the riverine transport of trace metals and metalloids (e.g. Pb, As, Cr, Co) [50,51]. It has been highlighted that Fe (oxy) hydroxides act as essential carriers for various (toxic) trace metals and the growth and agglomeration of Fe (oxy) hydroxides in stream will settle out in the slow-flowing sections of rivers, lakes, reservoirs or estuaries, co-precipitated with trace metals [52,53]. These deposits may, however, be remobilized during the flooding event because of the wet-dry cycles that may convert the oxidizing and reducing conditions in the riparian zones via alteration of Fe/Mn dynamics [54]. These processes may further facilitate the mobility of the redox-dependent trace metals together with their speciation and bioavailability, which would certainly have potential effects on the aquatic ecosystem [55]. However, it is still difficult to determine exactly how the impulse TDFe export influence the relative ecological processes in the boreal catchment and relevant ecosystems based on existing data. Further research is still needed to explore its environmental impacts in the future.

4. Conclusion

This study illustrates that the flooding event is in an essential position to TDFe transportation in the boreal forest catchment. The concentration of TDFe averaged at 0.24 mg/L with a trend of significant increase during EFE compared with that in RFS (0.20 mg/L) and BFP (0.15 mg/L), which was largely upon to hydrological connection to the riparian wetlands. However, the forest river may not be the major donator of TDFe to the Songhua River during EFE due to its relatively low concentration. The speciation of TDFe was dominated by Fe(III) at low molecular weight during all the monitored periods, accounting for more than 60% of total concentration during both EFE and RFS and over 50% during BFP. The variation of TDFe concentration and speciation during EFE was strongly correlated with the quantity and quality of DOM in the river water. Furthermore, TDFe may chiefly export as Fe(III)-DOM complexes accompanied by the transport and bioavailability of nutrient and trace metal which may further influence the water quality in the catchment due to its stability and transportability.

Acknowledgements

Funding support is gratefully acknowledged from National Nature Science Foundation of China (Grant: 41702370; 51408109), Jilin Provincial Research Foundation, China (Grant: 20170520080JH; 20160520078JH) and the Fundamental Research Funds for the Central Universities (Grant: 2412016KJ030).

References

[1] P.W. Boyd, M.J. Ellwood, The biogeochemical cycle of iron in the ocean, Nat. Geosci., 3 (2010) 675–682.

[2] S. Sarkkola, M. Nieminen, H. Koivusalo, A. Laurén, P. Kortelainen, T. Mattsson, M. Palviainen, S. Piirainen, M. Starr, L. Finér, Iron concentrations are increasing in surface waters from forested headwater catchments in eastern Finland, Sci. Total Environ., 463 (2013) 683–689.

[3] E. Orlowska, A. Roller, M. Pignitter, F. Jirsa, R. Krachler, W. Kandioller, B.K. Keppler, Synthetic iron complexes as models for natural iron-humic compounds: Synthesis, characterization and algal growth experiments, Sci. Total Environ., 577 (2017) 94–104.

[4] R.J. Yang, S. Han, S.L. Qu, X.C. Wang, Capacity of humic substances to complex with iron at different salinities in the Yangtze river estuary and east China sea, Sci. Rep., 7 (2017) 1381.

[5] K. Suzuki, A. Hattori-Saito, Y. Sekiguchi, J. Nishioka, M. Shigemitsu, T. Isada, H. Liu, R.M.L. Mckay, Spatial variability in iron nutritional status of large diatoms in the Sea of Okhotsk with special reference to the Amur River discharge, Biogeosciences, 11 (2014) 2503–2517.

[6] J. Nishioka, T. Nakatsuka, K. Ono, Y.N. Volkov, A. Scherbinin, T. Shiraiwa, Quantitative evaluation of iron transport processes in the sea of Okhotsk, Prog. Oceanogr., 126 (2014) 180–193.

[7] T. Nakanowatari, T. Nakamura, K. Uchimoto, J. Nishioka, J. Mitsudera, M. Wakatsuchi, Importance of Ekman transport and gyre circulation change on seasonal variation of surface dissolved iron in the western subarctic North Pacific, J. Geophy. Res. - Oceans, 122 (2017) 4364–4391.

[8] J.N. Guan, B.X. Yan, H. Zhu, L.X. Wang, D.A. Liu, L. Cheng, Flux characteristics of total dissolved iron and its species during extreme rainfall event in the midstream of the Heilongjiang River, J. Environ. Sci., 30 (2015) 74–80.

[9] J.N. Guan, B.X. Yan, X. Yuan, Variations of total dissolved iron and its impacts during an extreme spring flooding event in the Songhua River, J. Geochem. Explor., 166 (2016) 27–32.

[10] H. Laudon, M. Berggren, A. Agren, I. Buffam, K. Bishop, T. Grabs, M. Jansson, S. Kohler, Patterns and dynamics of dissolved organic carbon (DOC) in boreal streams: the role of processes, connectivity, and scaling, Ecosystems, 14 (2011) 880–893.

[11] C. Chen, J.J. Dynes, J. Wang, D.L. Sparks, Properties of Fe-organic matter associations via coprecipitation versus adsorption, Environ. Sci. Technol., 48 (2014) 13751–13759.

[12] Y.K. Henneberry, T.E.C. Kraus, P.S. Nico, W.R. Horwath, Structural stability of coprecipitated natural organic matter and ferric iron under reducing conditions, Org. Geochem., 48 (2012) 81–89.

[13] S.M. Ilina, F. Poitrasson, S.A. Lapitskiy, Y.V. Alekhin, J. Viers, O.S. Pokrovsky, Extreme iron isotope fractionation between colloids and particles of boreal and temperate organic-rich waters, Geochim. Cosmochim. Ac., 101 (2013) 96–111.

[14] L. Björkvald, I. Buffam, H. Laudon, C. Mörth, Hydrogeochemistry of Fe and Mn in small boreal streams: The role of seasonality, landscape type and scale, Geochim. Cosmochim. Ac., 72 (2008) 2789–2804.

[15] G.A. Weyhenmeyer, Y.T. Prairie, L.J. Tranvik, Browning of boreal freshwaters coupled to carbon-iron interactions along the aquatic continuum, PLoS One, 9 (2014) e88104.

[16] J.N. Guan, B.X. Yan, L.X. Wang, H. Zhu, L. Cheng, Variation in total dissolved iron output and iron species during extreme rainfall events, Clean-Soil, Air, Water, 6 (2016) 624–630.

[17] J.N. Guan, B.X. Yan, Y.Y. Xu, L.X. Wang, H. Zhu, Characteristics of total dissolved iron output and its species during different flood events in the Songhua River, Fresen. Environ. Bull., 24 (2015) 1169–1175.

[18] S.K. Oni, T. Tiwari, J.L.J. Ledesma, Local-and landscape-scale impacts of clear-cuts and climate change on surface water dissolved organic carbon in boreal forests, J. Geophys. Res.- Biogeo., 120 (2015) 2402–2426.

[19] J.L. Ledesma, M.N. Futter, H. Laudon, C.D. Evans, S.J. Köhler, Boreal forest riparian zones regulate stream sulfate and dissolved organic carbon, Sci. Total Environ., 560 (2016) 110–122.

[20] X. Pan, B. Yan, M. Yoh, L. Wang, X. Liu, Temporal variability of iron concentrations and fractions in wetland waters in Sanjiang Plain, Northeast China, J. Environ. Sci., 22 (2010) 968–974.

[21] C.J. Borman, B.P. Sullivan, C.M. Eggleston, P.J.S. Colberg, Is iron redox cycling in a high-altitude watershed photochemically or thermally driven? Chem. Geol., 269 (2010) 33–39.

[22] A. Zsolnay, E. Baigar, M. Jimenez, B. Steinweg, F. Saccomandi, Differentiating with fluorescence spectroscopy the sources of dissolved organic matter in soils subjected to drying, Chemosphere, 38 (1999) 45–50.

[23] D.M. McKnight, Spectrofluorometric characterization of dissolved organic matter for indication of precursor organic material and aromaticity, Limnol. Oceanogr., 46 (2001) 38–48.

[24] A. Huguet, L. Vacher, S. Relexans, S. Saubusse, J.M. Froidefond, E. Parlanti, Properties of fluorescent dissolved organic matter in the Gironde Estuary, Org. Geochem., 40 (2009) 706–719.

[25] S. Inamdar, S. Singh, S. Dutta, L. Delphis, M. Mitchell, D. Scott, H. Bais, P. Mchale, Fluorescence characteristics and sources of dissolved organic matter for stream water during storm events in a forested mid-Atlantic watershed, J. Geophys. Res.- Biogeo. 116 (2011) G03043.

[26] H.V.M. Nguyen, M.H. Lee, J. Hur, M.A. Schlautman, Variations in spectroscopic characteristics and disinfection byproduct formation potentials of dissolved organic matter for two contrasting storm events, J. Hydrol., 481 (2013) 132–142.

[27] L. Yang, S.W. Chang, H.S. Shin, J. Hur, Tracking the evolution of stream DOM source during storm events using end member mixing analysis based on DOM quality, J. Hydrol., 523 (2015) 333–341.

[28] S.A. Walker, R.M.W. Amon, C.A. Stedmon, Variations in high-latitude riverine fluorescent dissolved organic matter: A comparison of large Arctic rivers, J. Geophys. Res: Biogeo., 118 (2013) 1689–1702.

[29] A. Guarch-Ribot, A. Butturini, Hydrological conditions regulate dissolved organic matter quality in an intermittent headwater stream. From drought to storm analysis, Sci. Total Environ., 571 (2016) 1358–1369.

[30] T.M. Adyel, C.E. Oldham, M.R. Hipsey, Storm event-scale nutrient attenuation in constructed wetlands experiencing a Mediterranean climate: A comparison of a surface flow and hybrid surface-subsurface flow system, Sci. Total Environ., 598 (2017) 1001–1014.

[31] G.H. Zhou, B.B. Sun, D.M. Zeng, H.L. Wei, Z.Y. Liu, B.M. Zhang, Hydrogeochemical characteristics of major estuaries in eastern China: Physiochemical indicators and soluble element concentrations of river water, Geoscience, 39 (2012) 1028–1042.

[32] E.S. Kritzberg, A.B. Villanueva, M. Jung, H.E. Reader, Importance of boreal rivers in providing iron to marine waters, PloS One 9 (2014) e107500.

[33] C. Abesser, R. Robinson, C. Soulsby, Iron and manganese cycling in the storm runoff of a Scottish upland catchment, J. Hydrol., 326 (2006) 59–78.

[34] C.R. Cánovas, M. Olías, J.M. Nieto, A.M. Sarmiento, J.C. Cerón, Hydrogeochemical characteristics of the Tinto and Odiel Rivers (SW Spain). Factors controlling metal contents, Sci. Total Environ., 373 (2007) 363–382.

[35] D.A. Burns, J.J. Mcdonnell, R.P. Hooper, N.E. Peters, J.E. Freer, C. Kendall, K. Beven, Quantifying contributions to storm runoff through end-member mixing analysis and hydrologic measurements at the Panola Mountain Research Watershed (Georgia, USA), Hydrol. Process, 15 (2001) 1903–1924.

[36] G.Y. Chi, X. Chen, Y. Shi, T.H. Zheng, Forms and profile distribution of soil Fe in the Sanjiang Plain of Northeast China as affected by land uses, J. Soil. Sediment, 10 (2010) 787–795.

[37] L.J. Bracken, J. Wainwright, G.A. Ali, D. Tetzlaff, M.W. Smith, S.M. Reaney, A.G. Roy, Concepts of hydrological connectivity: research approaches, pathways and future agendas, Earth-Sci. Rev., 119 (2013) 17–34.

[38] H. Laudon, L. Kuglerová, R.A. Sponseller, M. Futter, A. Nordin, K. Bishop, T. Lundmark, G. Egnell, A.M. Ågren, The role of biogeochemical hotspots, landscape heterogeneity, and hydrological connectivity for minimizing forestry effects on water quality, Ambio., 45 (2016) 152–162.

[39] B.X. Yan, J.N. Guan, V. Shesterkin, H. Zhu, Variations of dissolved iron in the Amur River during an extreme flood event in 2013, Chinese Geogr. Sci., 26 (2016) 679–686.

[40] R. Angelico, A. Ceglie, J.Z. He, Y.R. Liu, G. Palumbo, C. Colombo, Particle size, charge and colloidal stability of humic acids coprecipitated with ferrihydrite, Chemosphere, 99 (2014) 239–247.

[41] J. Awad, J.V. Leeuwen, D. Abate, M. Pichler, E. Bestland, D.J. Chittleborough, N. Fleming, J. Cohen, J. Liffner, M. Drikas, The effect of vegetation and soil texture on the nature of organics in runoff from a catchment supplying water for domestic consumption, Sci. Total Environ., 529 (2015) 72–81.

[42] D.N. Kothawala, X. Ji, H. Laudon, A.M. Ågren, The relative influence of land cover, hydrology, and in-stream processing on the composition of dissolved organic matter in boreal streams, J. Geophys. Res.- Biogeo., 120 (2015) 1491–1505.

[43] N. Catalán, H. Ortega, H. Gröntoft, T.G. Hilmarsson, S. Bertilsson, P. Wu, O. Levanoni, K. Bishop, A.G. Bravo, Effects of beaver impoundments on dissolved organic matter quality and biodegradability in boreal riverine systems, Hydrobiologia, 793 (2017) 135–148.

[44] J. Schelker, K. Öhman, S. Löfgren, H. Laudon, Scaling of increased dissolved organic carbon inputs by forest clear-cutting - What arrives downstream? J. Hydrol., 508 (2014) 299–306.

[45] M. Zamparas, I. Zacharias, Restoration of eutrophic freshwater by managing internal nutrient loads, A review, Sci. Total Environ., 496 (2014) 551–562.

[46] X.F. Li, L.J. Hou, M. Liu, X.T. Hu, Evidence of nitrogen loss from anaerobic ammonium oxidation coupled with ferric iron reduction in an intertidal wetland, Environ. Sci. Technol., 49 (2015) 11560–11568.

[47] A. Sundman, T. Karlsson, S. Sjöberg, P. Persson, Impact of iron-organic matter complexes on aqueous phosphate concentrations, Chem. Geol., 426 (2016) 109–117.

[48] Y.H. Xiao, L. Hoikkala, V. Kasurinen, M. Tiirola, P. Kortelainen, A.V. Vähätalo, The effect of iron on the biodegradation of natural dissolved organic matter, J. Geophys. Res.- Biogeo., 121 (2016) 2544–2561.

[49] J.C. Clément, J. Shrestha, J.G. Ehrenfeld, P.R. Jaffe, Ammonium oxidation coupled to dissimilatory reduction of iron under anaerobic conditions in wetland soils, Soil Biol. Biochem., 37 (2005) 2323–2328.

[50] T. Karlsson, P. Persson, Complexes with aquatic organic matter suppress hydrolysis and precipitation of Fe(III), Chem. Geol., 322 (2012) 19–27.

[51] J.M. Blake, S.C. Peters, A. Casteel, Zinc, copper, nickel, and arsenic monitoring in natural streams using in-situ iron-manganese oxide coated stream pebbles, J. Geochem. Explor., 158 (2015) 168–176.

[52] E. Neubauer, S.J. Köhler, F. von der Kammer, H. Laudon, T. Hofmann, Effect of pH and stream order on iron and arsenic speciation in boreal catchments, Environ. Sci. Technol., 47 (2013) 7120–7128.

[53] T. Wällstedt, L. Björkvald, H. Laudon, H. Borg, C.M. Mörth, Landscape control on the hydrogeochemistry of As, Co and Pb in a boreal stream network, Geochim. Cosmochim. Ac., 211 (2016) 194–213.

[54] F. Lidman, Å. Boily, H. Laudon, S.J. Köhler, From soil water to surface water-how the riparian zone controls element transport from a boreal forest to a stream, Biogeosciences, 14 (2017) 3001–3014.

[55] S.M. Shaheen, E.E. Kwon, J.K. Biswas, F.M.G. Tack, Y.S. Ok, J. Rinklebe, Arsenic, chromium, molybdenum, and selenium: Geochemical fractions and potential mobilization in riverine soil profiles originating from Germany and Egypt, Chemosphere, 180 (2017) 553–563.